Fabric Membranes Cutting Pattern

Bernard Maurin[1] and René Motro[2]

[1] Laboratoire de Mécanique et Génie Civil `maurin@lmgc.univ-montp2.fr`
[2] Laboratoire de Mécanique et Génie Civil `motro@lmgc.univ-montp2.fr`

1 Introduction

Tensile fabric membrane design implies successive stages, each of one related to particular problems requiring well adapted approaches and appropriated results.

The first step of the analysis deals with the form-finding process that corresponds with the coupling in lightweight structures between the form (geometry) and the forces (initial tension). The objective is to determine the shape of the membrane associated to its prestress distribution. A good control on the tension in the fabric must be obtained in order to have suitable stresses, for instance that ensure the absence of compressive zones.

The following stage focuses on the realization of the tensile membrane calculated during the form-finding. More precisely, the objective is to determine the starting configuration (set of plane *strips*) which, once assembled on the site according to specified anchoring conditions, will lead closely to the required surface, that is to say to the theoretical one (target strip) calculated during the shape-finding procedure with its associated characteristics of form and prestress. The erection process indeed generated deformations on each strip that will define in the end a mechanically equilibrated geometry coupled with a prestress distribution. The purpose is to minimize the differences between the target state and the therefore obtained state. It corresponds with the *cutting pattern stage*.

In case of low deviances, the prejudice will be essentially aesthetic such as disgraceful folds (Fig. 1 left) but, in case of higher differences, the integrity of the whole structure could be affected since large membrane zones may be less or not tensioned, this leading to major risk of failure (wind fluttering, horizontal areas with stagnant rain water..., Fig. 1 right). The cutting pattern necessitates the specification of the surface cutting lines also called *strip edges*. This procedure has to take into consideration several parameters likewise technology, geometry, mechanics and aesthetics.

Each strip being so identified, the designer must next calculate the associated

plane fabric cutting patterns. Most of the used methods split the process into two different stages. In the first one, the 3D strip is flattened onto a projection plane; in the second, the pretension of the membrane is considered so as to reduce its dimensions.
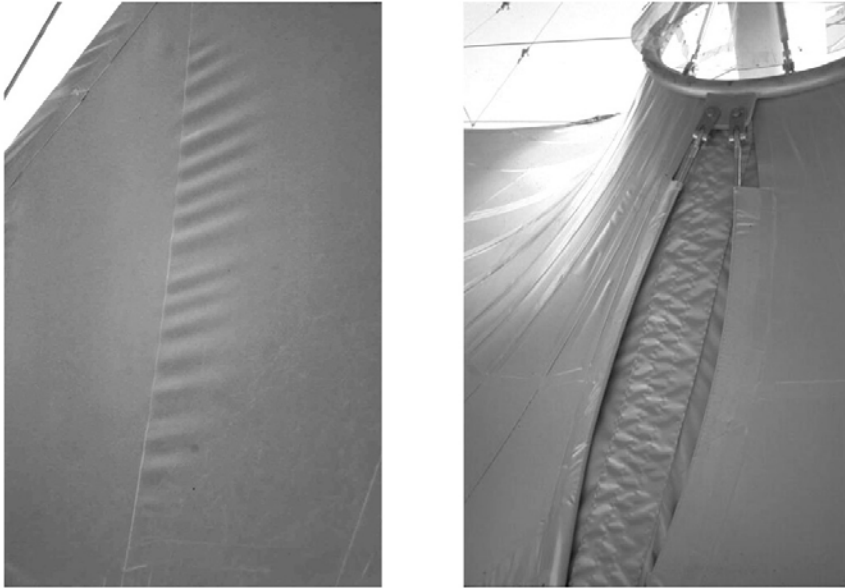

Fig. 1. Folds at strip edges; compressive zones

2 Strip Edges Determination

This process results in determining the balance between various, and sometimes opposite, requirements.

2.1 Technological Issues

The design must firstly take into account the maximum strip widths in connection with the products available from fabric manufacturers. Generally, membranes are supplied in the form of 2m width rolls [5]. After cutting, the strips are assembled by thermo-welding (fusing of the material between high frequency electrodes and pasted by applying a pressure); the resulting membrane is next transported to the erection site.

2.2 Geometrical Issues

Some designers consider as necessary to have strip edges along geodesic curves ([2] and [14]). It allows indeed, in the particular case of surfaces that are developable onto a plane (on the mathematical meaning), to generate straight lines in accordance with an economical objective of minimal material wastes. This approach may however be relativized since, in the case of double curvature geometries, the surfaces are not developable: we know that such operation leads to unavoidable distortions. It is then judicious to use low dimension strips on a surface zone with high total curvatures. A numerical method devoted to the calculation of membrane curvatures is presented in appendix. Nevertheless, this consideration has to be balanced with a resulting increase of the cutting operations and welding lengths and therefore of the total cost.

2.3 Mechanical Issues

The production of the fabric does not end in a perfect isotropy between the warp and weft directions (higher strength and stiffness for the warp) even if improvements in production processes aim to reduce this difference. The low shear strength of the fabric has also to be taken into account. Thus, an ideal configuration will be related to the positioning of the strip edges, that correspond after cutting approximately with the warp direction, along the direction of the main forces, that is to say the maximum principal stresses. In that case, the fabric weft is thus turned on to the minimum stresses directions with resulting shear forces close to zero. All of these theoretical considerations have however to be balanced with practical aspects: inexistence of exact solution, knowledge of stresses due to the initial stresses in the fabric and to climatic effects. If the action of wind is paramount (pressure normal to the surface), then the directions of maximum stresses correspond with the directions of the membrane maximum curvatures. For snow (vertical action) the answer is much more complex but some basic cases such as the radial positioning of the strip edges at the top of anchoring masts (Fig. 2). In addition to these requirements dealing with the surface, others considerations are related to the membrane edges. Since the initial pretension is applied by progressively tensioning edge cables, it is necessary that strip edges be orthogonal to these cables.
However, so as to point out the problems associated to particular situations, we quote the case of the design of Mina Valley tents in Mecca build for pilgrims [10]. The project, realised in two stages in 1997/98, is composed of 40000 tents with a rectangular frame (from 4x4m to 8x12m) with a vertical mast at middle. The membranes build during the first stage are based upon the basic radial positioning of strip edges, but the difficulties in tensioning the fabric with the mast have lead to prohibited folds on the surface. The designers of the second team have then decided to set the strip edges parallel to the anchoring sides.
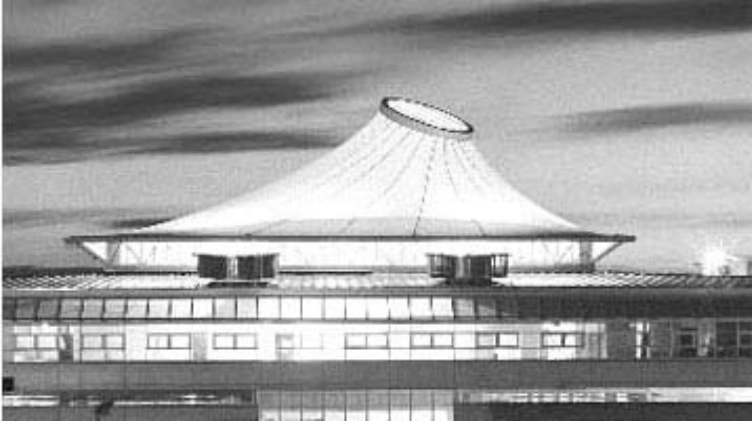
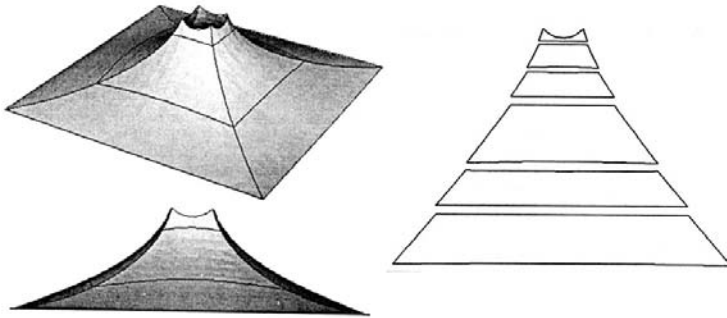**Fig. 2.** Radial strip edges

Fig. 3. Strips used for the Mina project stage 2

It was allowed by the absence of snow and has resulted in the vanishing of the folds (Fig. 3).

We emphasize herewith on the fact that small structures design may generate more difficulties than wider membranes design since the dimension of the fabric rolls appears as important with reference to the dimensions of the structure.

2.4 Aesthetical Issues

The approach could however be modified when architects play a role. Their creativity may for instance leads to the making of geometric drawings by using fabric samples of different colours. Moreover, since the visual perception of the surface is dependant on the strip edges positioning, mainly at night, this architectural feature could lead to specific patterning strategies.

3 Cutting Shapes Determination

3.1 Background

Before presenting several used methods, we aim to point out some significant principles.

Since the objective is to have a good adequacy between the target state and the real state, it is thus necessary for each strip to evaluate the result in the light of the morphological parameters of forms and forces:

- If the geometry of the strip put into place is close to those theoretically determined during the form-finding stage, we will say that it exists a *geometrical equivalence* between the two strips. However, one point has to be respected: an edge belonging to two strips must have the same length on the plane cutting shapes so as to allow their future assembly.

- Similarly, if the prestress field generated in the strip is close to the required one, the *sthenical equivalence* is ensured. We may observe that it implies the perfect knowledge of the selfstress state determined during the form-finding process.

Nevertheless, these two principles only represent a virtual reality since it is illusory to expect a complete equivalence but very particular cases. A patterning method without taking into account all the geometric and sthenic data will however not offer the possibility to have an optimal solution to the problem. The same comment is also relevant if these considerations are not seen as indissociable and so envisaged as two separate steps (flattening and then reduction). We remark that, as far as we can know, most of the used methods are based upon such splitting.

Let's now have a look on the existing flattening processes.

The first technique is the *simple triangulation method* (Fig. 4). The 3D strip (a) determined by form-finding is mapped with a series of triangles between the longest edges, leading to the geometry (b). The obtained triangles are next successively flattened onto a plane by keeping identical the lengths of their sides (c). Since this method is quick and easy to apply, it is at the core of numerous CAD tools.
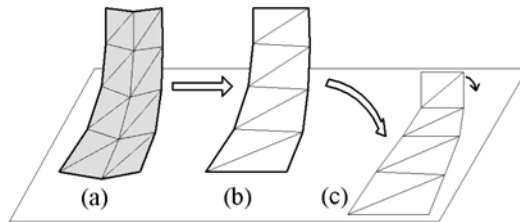

Fig. 4. Simple triangulation method

We may however note that it does not take into consideration a lot of points: those located inside the strip and some on top and bottom edges. Its use therefore requires caution so as to avoid important errors.

Several authors have thus proposed improved processes. L. Gründig has put forward a method which takes into account all the points belonging to the strip edges [7]; this objective being also one of H. Tsubota's aims [13]. In both cases, the geometry of edges is calculated by using minimization error processes. We may regret that data of internal points are still avoided. The method proposed by T. Shimada ([12] and [1]) offers some improvements on that purpose. It consists in determining a plane domain composed of triangular surface elements which, once transformed into the 3D strip, leads to a minimal strain energy. The material characteristics are used in the mechanical formulation. However, parameters related to the prestress of the membrane are not considered.

In each situation, the development of the strip must be followed by an operation so as to take into account the initial stresses. Three main strategies may be pointed up:

- The strip is not modified. Stresses in the fabric are generated by the displacements of anchoring zones (mast erection, shortening of edge cable lengths...).

- If the strip is triangulated, every element is reduced along two directions in relation with the selfstresses determined by shape-finding. In the case of uniform stresses within the strip (minimal area surface for instance) the solution in not difficult. On the contrary, specific methods are to be used to determine an accurate result.

- The most commonly used technique results in considering a reduction scale factor for the developed shape. The designer applies it generally along the longer direction of the strip (the warp direction, with a factor from 2 to 3%) and the transverse reduction along the weft is obtained during the strips assembling (bilayer of the welded zone close to 2cm width).

The experience and a good knowledge of the material, mainly obtained by mechanical testing (stiffness, creep... [6]), play nevertheless a major role in these methods and the designer must proceed carefully.

If every cutting pattern process unavoidably leads to errors, we may remark that the greatest part of them are directly related to the splitting of the technique into two separate operations of flattening (for the geometry) and reduction (for the prestress). Hence, it appears that a better solution obviously relies in an *integrated approach* which takes into account at the same time the considerations of form, forces and material. The target state has to be determined in a comprehensive process without splitting of these parameters. Several research teams have thus proposed innovative patterning methods based upon such integrated approach. We may quote the works of J. Kim [8] and the method developed at the Mechanics and Civil Engineering Laboratory at Montpellier University and called *stress composition* method [9].

3.2 Stress Composition Method

We consider a 3D target strip Ω^{L} calculated by form-finding process and with every elementary prestress tensor known $\{\sigma_{loc}^{\mathrm{ff}}\}_L = \{\sigma_x\ \sigma_y\ \sigma_{xy}\}_{\mathrm{L}}$. The method relies in the determination of the plane cutting shape Ω^0 such as its exact transformation into Ω^{L} (that is to say by considering the geometrical equivalence as respected) generates these stresses (i.e. the sthenical equivalence as an objective). We will in the end go back on the relevance of this starting assumption.

On that purpose, a starting domain Ω^* is defined (determined by the orthogonal projection of the target strip on the development plane) and is deformed into Ω^{L} hence generating the prestress $\{\sigma_{loc}\}_{\mathrm{L}}$. If these values are different from $\{\sigma_{loc}^{\mathrm{ff}}\}_L$ then Ω^* is modified into Ω^0, so as the resulting stresses $\{\sigma_{loc}^{\mathrm{mod}}\}_*$ balance the observed deviation (Fig. 5). The calculation of the tensor $\{\sigma_{loc}\}_{\mathrm{L}}$ is achieved in accordance with the hypothesis of large displacements. The mechanical characteristics of the fabric are taken into account during every transformation.
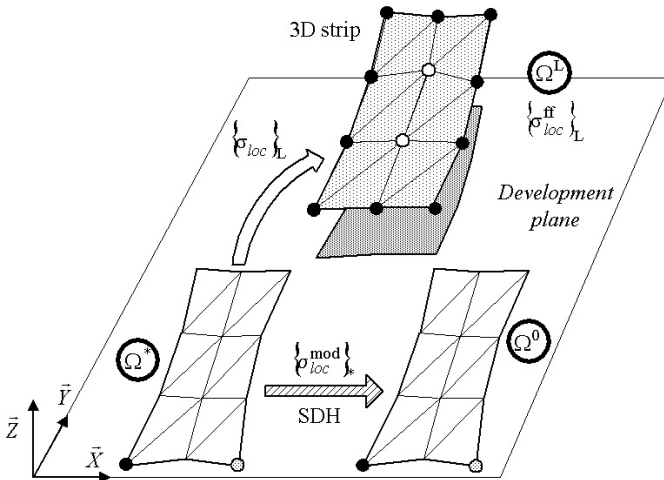

Fig. 5. Used configurations

The modification of Ω^* into Ω^0 is achieved according to the small displacements and small strains hypothesis (SDH), by acting on the boundary conditions of the frontier nodes of Ω^* in order to have $\{\sigma_{loc}^{\mathrm{mod}}\}_*$ close to the deviation $\{\sigma_{loc}\}_{\mathrm{L}} - \{\sigma_{loc}^{\mathrm{ff}}\}_{\mathrm{L}}$.

The associated displacement $\{d_{\mathrm{f}}^{\mathrm{mod}}\}_*^0$ (Fig. 6) may be determined with reference to the matrix relationship:

$$[A_\sigma]_* \{d_{\mathrm{f}}^{\mathrm{mod}}\}_*^0 = \{\sigma_{\mathrm{loc}}^{\mathrm{mod}}\}_* \tag{1}$$
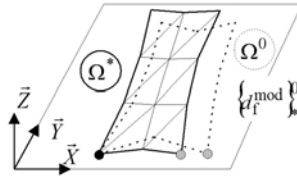
Fig. 6. Transformation of Ω^* into Ω^0

The equation is solved by using a least square method that provides a first approximate solution of Ω^0 called $\Omega^{0(1)}$. We consider next a second "starting" domain $\Omega^{*(2)} = \Omega^{0(1)}$; it allows therefore to calculate a second approximation $\Omega^{0(2)}$ of Ω^0. This iterative process constitutes the background of the stress composition method (Fig. 7).
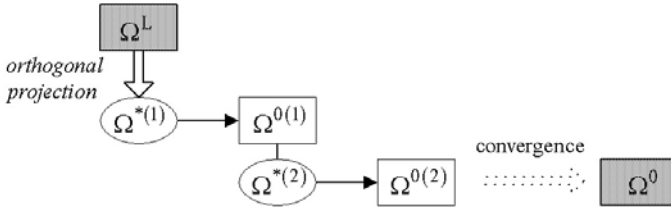

Fig. 7. Stress composition method

It converges in p iterations into the domain $\Omega^{0(\mathrm{p})}$ characterized by a stress deviation $\Delta\sigma_0^{\mathrm{L(p)}}$ according to:

$$\Delta\sigma_0^{\mathrm{L(p)}} \, \|\{\sigma_{loc}^{\mathrm{ff}}\}_{\mathrm{L}}\| = \|\{\sigma_{loc}^{\mathrm{ff}}\}_{\mathrm{L}} - \{\sigma_{loc}\}_{\mathrm{L}} + \{\sigma_{loc}^{\mathrm{mod(p)}}\}_*\| \qquad (2)$$

The sthenic convergence criterion is set by the designer accordingly to the required maximum value of $\Delta\sigma_0^{\mathrm{L(p)}}$. The vectorial norm $\| \ \|$ corresponds to the euclidian norm.

3.3 Application

The searched 3D strip belongs to a minimal area surface characterised by an isotropic and uniform prestress $\{\sigma_{loc}^{\mathrm{ff}}\}_{\mathrm{L}} = \{\sigma_0 \ \sigma_0 \ 0\}_{\mathrm{L}}$ with $\sigma_0 = 250 \, \mathrm{daN/m}$. The dimensions of the strip in plane projection are 10m x 2m with an elevation of 1m in the top vertex (Fig. 8). The mechanical features of the material are those of a manufactured fabric: warp direction Young modulus equal to 24900 daN/m and 23000 daN/m for the weft direction with Poisson coefficients 0,097 and 0,090.

The stress composition method converges in seven iterations with a stress distortion $\Delta\sigma_0^{\mathrm{L(7)}} = 3,70\%$ with reference to the target state.
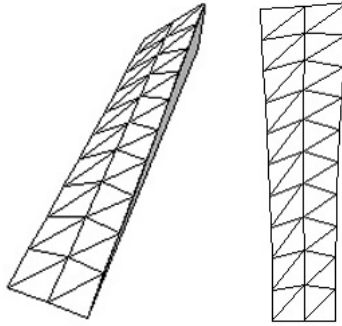
Fig. 8. Strip determined with the stress composition method

The following graph represents the values of the principal stresses σ_1 and σ_2 for every 40 triangular elements used for the modelling; the ideal solution is drawn by the horizontal line $\sigma_1 = \sigma_1 = \sigma_0 = 250$ daN/m (target state). We observe a regular stress distribution within the surface and the solution appears as quite satisfactory.
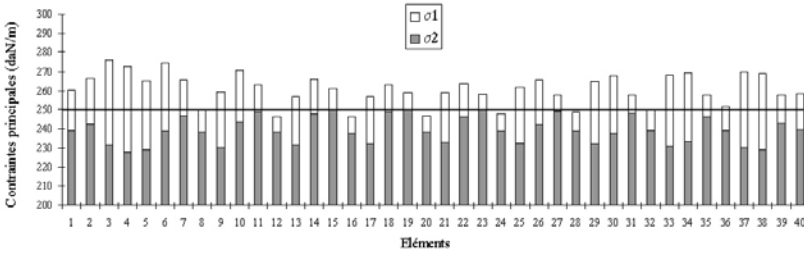

Fig. 9. Principal stresses obtained with the integrated method

If the same strip is now calculated with the simple triangulation method followed by a reduction, the determined shape may be characterised by a stress deviance $\Delta\sigma_0^{\mathrm{L}(7)} = 26,62\%$ (evaluated after remeshing the plane domain with 40 triangular elements by adding internal nodes without altering the geometry of edges).

The values of the resulting principal stresses are presented in the following graph.

We point out that, when all the geometry of the domain is not taken into consideration likewise during the mapping with simple triangulation, increasing deviances occur. Such result is however not so surprising. A more detailed analysis of the graph allows noticing a higher distortion between the principal stresses for the elements located in the top zone of the surface (right part of the graph). A possible explanation relies in the fact that these elements are
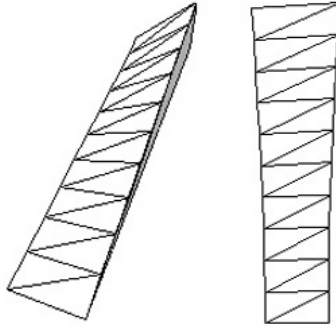
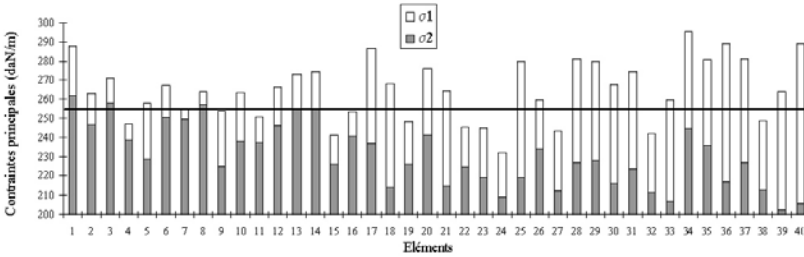**Fig. 10.** Strip determined with simple triangulation method

Fig. 11. Principal stresses obtained with simple triangulation method

subjected to the highest strains, which may generate shear forces and thus differences between the principal stresses.

4 Modelling of the Strip Prestressing

All the cutting pattern methods previously presented are based upon an implicit hypothesis: the plane strip will be exactly transformed into the target 3D strip, that is to say the surface determined by form-finding will be, in the end, exactly obtained. Some comments may be pointed up. Firstly, we notice that such postulate is a strong one with reference to possible consequences. However it must also be kept in mind the difficulty to avoid such assumption in order to be able to determine the cutting shapes. Nevertheless, a rigorous process has to check both the geometrical and sthenical deviances between the target membrane and those obtained after prestressing the assembled membrane in the site. Cutting pattern and prestressing stages may be thus regarded as a "back and return" operation.

The modelling of the prestressing operation could be envisaged according to two levels of complexity:

- A global approach in which the designer studies the deployment of the whole

membrane. Beside the difficulty in writing the mechanical formulations (large displacements context), main difficulties are associated with the modelling of the assembled membrane (mainly the folds [4]) and various interaction phenomena (friction between fabric and tensioning edge cables, sequence of erection...).

- A local strategy aiming to analyze separately each tensioned strip. Even if its adequacy with the reality is somehow hypothetic, this approach is more easily achievable and may leads to relevant and pertinent informations. One possible method is presented in the following paragraphs.

It consists in considering the transformation of Ω^0 into a tensile configuration by prescribing nodal displacements on the boundary (nodes on strip edges) until a perfect coincidence with the target strip is obtained. This prestressing leads in p steps to a domain $\Omega^{\mathcal{P}}$ with an estimated matching with Ω^L by considering both the form (geometrical equivalence of inner points) and the stress distribution (sthenical equivalence). If a good correspondence is verified, we may thus conclude in the good adequacy of the cut shape.

The formalism relies on a total lagrangian formulation considering the reference configuration Ω^0 and successive steps. The transformation between two steps (for instance from Ω^1 to Ω^2, assumed as very close) is achieved with an increment of the nodal displacements $\{d\}_1^2$ (Fig. 12).
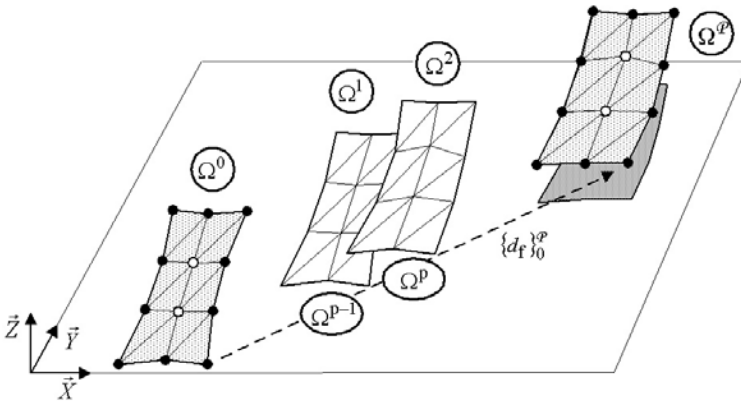

Fig. 12. Prestressing of the strip Ω^0

By considering Ω^1 as already determined (equilibrium obtained), Ω^2 must necessarily verify the virtual works theorem [3]:

$$\delta W_0^{2-1} = \langle \delta d \rangle_0 \, [k_T]_0^2 \, \{d\}_1^2 = 0 \tag{3}$$

The tangent stiffness matrix appears in this writing; it could be splitted according to its linear, non linear (initial displacements) and geometric components:

$$[k_T]_0^2 = [k_L]_0^2 + [k_{NL}]_0^2 + [k_\sigma]_0^2 \tag{4}$$

The non linear problem may be iteratively solved with the Newton-Raphson method. When the convergence is obtained (low residual on $\Omega^{\mathcal{P}}$), it is then possible to determine a level of geometric distortion $\Delta g_{\mathrm{L}}^{\mathcal{P}}$ related to the deviance in internal nodes positions and a level of sthenic distortion $\Delta\sigma_{\mathrm{L}}^{\mathcal{P}}$.

We consider as an illustrative example the prestressing of the strip previously calculated with the integrated method. The figure 13 represents the target strip Ω^{L} and the associated plane domain Ω^0. In ten incrementation steps, it leads to a configuration $\Omega^{\mathcal{P}} = \Omega^{10}$ close to Ω^{L}; we verify moreover that $\Delta g_{\mathrm{L}}^{10} = 0,21\%$. This result is in accordance with the geometrical equivalence used during the patterning process. We note in addition that the distortion between the target and the obtained stresses is $\Delta\sigma_{\mathrm{L}}^{10} = 3,81\%$ (with a distribution of principal stresses on $\Omega^{\mathcal{P}}$ close to those represented in Fig. 9).
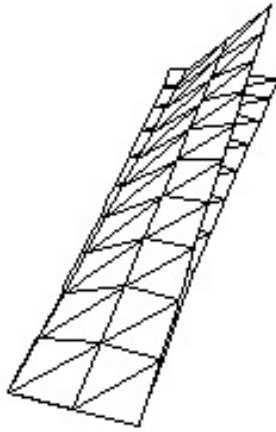

Fig. 13. "Back and return"

A second illustration deals with the analysis of a strip extracted from a minimal area shape ("chinese hat" type) with dimensions 20m and 4m for circle diameters and 4m for the height. The plane cutting shape determined with the integrated method is characterized by an error of of 10,48% for the pretension and 0,92% for the geometry (Fig. 14 left). A calculation with the simple triangulation method leads to higher deviances with approximately 45% for stresses (Fig. 14 right). Such result is however only the consequence of the imperfections of this process that avoids a lot of points inside the strip and an important boundary point located on the bottom circle.

The presented two tests allow to point out the importance of the errors due to the flattening of a doubly curved surface. They have to be considered in parallel with the possible errors generated during the form-finding stage. It emphasizes on the fact that distortions generated during the patterning stage play the main role.
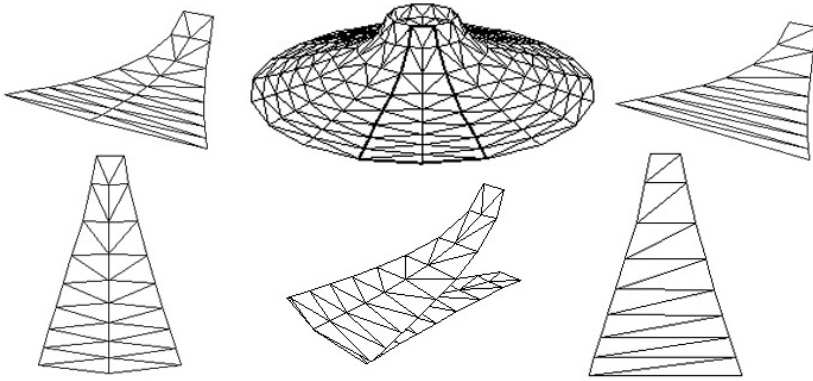
Fig. 14. Strip determined with integrated method (left) and simple triangulation (right)

5 Conclusion

The cutting pattern of strips for tensile membranes is more often achieved by considering the stage of flattening and the stage of reduction as separated. Instead of this splitting, it can be used an integrated approach such as the stress composition method that takes into account the characteristics of the fabric. It allows to take more appropriately into consideration the coupling between the parameters of form, forces and material and, thus, to respect the different requirements of technology, geometry, mechanics and architecture.

6 Appendix: Membrane Local Curvatures Computation

Tensile fabric membrane design implies several stages which require the use of geometrical characteristics.
Firstly, the designer has to verify that the shape calculated by form-finding analysis satisfies numerous requirements.

- The maximum curvature radius must be less than prescribed values. It traduces the relationship between the membrane stiffness at one point and the curvatures; therefore the behaviour of the structure when climatic loads are active. This requirement could affect the membrane itself and reinforcing edge cables as well. Most generally, the limits are defined by national codes. For instance, in France, the membrane maximum curvature radius is 35m and the edge cable maximum curvature radius is 25m.
- The minimal slope must be superior to specified values. The objective is to avoid too "horizontal" areas where rainwater could possibly stay and thus damage the fabric because of local lower stiffness. A suitable criteria may be put forward by determining at the studied zone the vector perpendicular to the surface.

Secondly, a geometrical analysis is necessary so as to provide the designer with important parameters during the cutting pattern procedure:

- The value of the gaussian curvature is associated to the difficulty to develop a curved surface onto a plane (flattening). The designer should take it into account so as to control the width of the strips over the membrane. Hence, a "map" representing the gaussian curvature value at every point of the surface could be a useful tool.
- The specification of the strip edges which divide the membrane is approached under several criteria. The use of geodesic curves could be of importance and therefore their calculation which imply numerous geometrical informations such as surface normal vectors.

The objective of this appendix is thus to submit a numerical approach devoted to the determination of membrane local curvatures. It deals with the case of mapped surfaces that define the height of the points as a function of the two other plane coordinates, that is to say $z = f(x, y)$ with f representing a bijection between z and the pair (x, y). In that case, theoretical relationships allow to calculate at every point the values of the mean and gaussian curvatures, and next, to determine the maximum and minimum curvature radii. We propose to solve all partial differential equations by using the polynomial shape functions of finite elements.

6.1 The Calculation Strategy

In the case of mapped surface, a vertical line with fixed x and y coordinates intersects the domain at only one point for which we can write the relationship $z = f(x, y)$.

For every surface it exists two orthogonal planes that define the principal curvature directions θ_1 and θ_2 associated to the main curvatures ρ_1 and ρ_2 (minimum and maximum values).

With function z it is then possible to calculate at every point the partial derivative terms [11]:

$$p = z_{,x} \; ; \; q = z_{,y} \; ; \; r = z_{,xx} \; ; \; s = z_{,xy} \text{ and } t = z_{,yy} \tag{5}$$

Thus the surface gaussian curvature G and the mean curvature H are defined by:

$$G = (rt - s^2)(1 + p^2 + q^2)^{-2} \text{ and}$$
$$H = (t(1 + p^2) - 2pqs + r(1 + q^2))(1 + p^2 + q^2)^{-3/2} \tag{6}$$

The curvatures radii R_1 and R_2 are next determined with:

$$G = \rho_1 \rho_2 \; ; \; H = 0,5(\rho_1 + \rho_2) \text{ and}$$
$$R_1 = \frac{1}{\rho_1} = (H + (H^2 - G)^{1/2})^{-1} \; ; \; R_2 = \frac{1}{\rho_2} = (H - (H^2 - G)^{1/2})^{-1} \tag{7}$$

The two principal directions θ_1 and θ_2 may be calculated according to the system (with $\mathcal{D} = tg\theta = \frac{dy}{dx}$):

$$\begin{cases} \mathcal{D}_1 + \mathcal{D}_2 = (-t(1+p^2) + r(1+q^2))(pqt - s(1+q^2))^{-1} \\ \mathcal{D}_1\mathcal{D}_2 = (s(1+p^2) - pqr)(pqt - s(1+q^2))^{-1} \end{cases} \quad (8)$$

And the components of vector $\overrightarrow{n}_s$ normal to the surface are:

$$\overrightarrow{n}_s(-hp \; ; \; -hq \; ; \; h) \text{ with } h = (1 + p^2 + q^2)^{-1/2} \quad (9)$$

In fact the main difficulty is related to the determination at every point of the function $z = f(x, y)$ and its partial derivatives. Thus, we propose to use finite element polynomial shape functions N in order to interpolate the geometry of the surface within the area "close to" a chosen point. The elevation z is written $z = N_i z_i$; the index i indicates a summation over the n nodes element ($i = 1$ to n). We note that a not too large surface surrounding a selected point can always be described as a mapped domain by using a local referential coordinate transfer.

Since partial derivative equations involve an order two for derivatives, the finite element must have at least a quadratic polynomial interpolation. We propose to use 6 nodes triangle (T6) and 9 nodes rectangle (R9) for a quadratic interpolation and 10 nodes triangle (T10) for a cubic interpolation. Theoretically, a higher interpolation degree should lead to more accurate results.

The associated standard elements are represented in Fig. 15 in their cartesian natural axis ξ and η that are used to define shape functions $N_i(\xi, \eta)$.
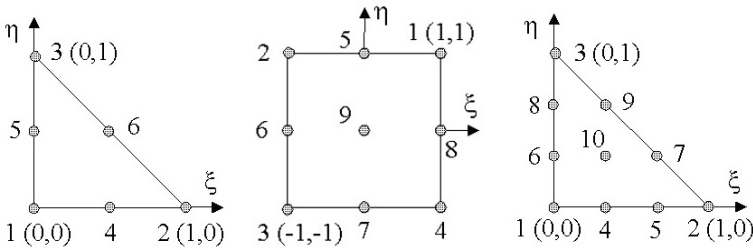

Fig. 15. Elements (T6, R9 and T10)

These elements are not dependent on those used for the mesh during the form-finding analysis. The only matching up parameter is the nodal coordinates of the discrete surface. The objective is to calculate the interpolated values:

$$p = N_{i,x} z_i \; ; \; q = N_{i,y} z_i \; ; \; r = N_{i,xx} z_i \; ; \; s = N_{i,xy} z_i \text{ and } t = N_{i,yy} z_i \quad (10)$$

We must write the jacobian matrix corresponding to the transformation between the standard element and the element over the surface and calculate

its determinant $D = N_{i,\xi}\, N_{i,\eta}\,(x_i y_j - x_j y_i)$ and its first derivatives:

$$\begin{cases} D_{,\xi} = (N_{i,\xi\xi}\, N_{j,\eta} + N_{i,\xi}\, N_{j,\xi\eta})\,(x_i y_j - x_j y_i) \\ D_{,\eta} = (N_{i,\eta\xi}\, N_{j,\eta} + N_{i,\xi}\, N_{j,\eta\eta})\,(x_i y_j - x_j y_i) \end{cases}$$

$$\begin{cases} (D^{-1})_{,\xi} = D^{-1}_{,\xi} = -D^{-2}\, D_{,\xi} \\ (D^{-1})_{,\eta} = D^{-1}_{,\eta} = -D^{-2}\, D_{,\eta} \end{cases} \tag{11}$$

If we calculate then the components of the inverse jacobian matrix:

$$a = \xi_{,x} = D^{-1}\, N_{i,\eta}\, y_i \;;\; b = \eta_{,x} = -D^{-1}\, N_{i,\xi}\, y_i \text{ and}$$
$$c = \xi_{,y} = -D^{-1}\, N_{i,\eta}\, x_i \;;\; d = \eta_{,y} = D^{-1}\, N_{i,\xi}\, x_i \tag{12}$$

The partial first derivatives are defined according to:

$$N_{i,x} = a\, N_{i,\xi} + b\, N_{i,\eta} \text{ and } N_{i,y} = c\, N_{i,\xi} + d\, N_{i,\eta} \tag{13}$$

And the partial second derivatives are:

$$\begin{cases} N_{i,xx} = a^2 N_{i,\xi\xi} + b^2 N_{i,\eta\eta} + 2ab N_{i,\xi\eta} + (aa_{,\xi} + ba_{,\eta})N_{i,\xi} \\ \quad + (ab_{,\xi} + bb_{,\eta})N_{i,\eta} \\ N_{i,xy} = ac N_{i,\xi\xi} + bd N_{i,\eta\eta} + (cb + ad)N_{i,\xi\eta} + (ca_{,\xi} + da_{,\eta})N_{i,\xi} \\ \quad + (cb_{,\xi} + db_{,\eta})N_{i,\eta} \\ N_{i,yy} = c^2 N_{i,\xi\xi} + d^2 N_{i,\eta\eta} + 2cd N_{i,\xi\eta} + (cc_{,\xi} + dc_{,\eta})N_{i,\xi} \\ \quad + (cd_{,\xi} + dd_{,\eta})N_{i,\eta} \end{cases} \tag{14}$$

With the following coefficients:

$$\begin{cases} a_{,\xi} = -D^{-1}_{,\xi} N_{i,\eta} y_i + D^{-1} N_{i,\xi\eta} y_i \\ a_{,\eta} = -D^{-1}_{,\eta} N_{i,\eta} y_i + D^{-1} N_{i,\eta\eta} y_i \\ b_{,\xi} = -D^{-1}_{,\xi} N_{i,\xi} y_i - D^{-1} N_{i,\xi\xi} y_i \\ b_{,\eta} = -D^{-1}_{,\eta} N_{i,\xi} y_i - D^{-1} N_{i,\xi\eta} y_i \end{cases}$$

$$\begin{cases} c_{,\xi} = -D^{-1}_{,\xi} N_{i,\eta} x_i - D^{-1} N_{i,\xi\eta} x_i \\ c_{,\eta} = -D^{-1}_{,\eta} N_{i,\eta} x_i - D^{-1} N_{i,\eta\eta} x_i \\ d_{,\xi} = -D^{-1}_{,\xi} N_{i,\xi} x_i + D^{-1} N_{i,\xi\xi} x_i \\ d_{,\eta} = -D^{-1}_{,\eta} N_{i,\xi} x_i + D^{-1} N_{i,\xi\eta} x_i \end{cases} \tag{15}$$

Since derivatives $N_{,\xi} \ldots N_{,\xi\eta}$ are dependent on ξ and η values, the calculation could be achieved at any chosen point within the element, for instance a point located in the middle of two nodes.

6.2 Applications

Test

The first application allows the verification of formulations. It deals with an hyperbolic paraboloid (HP) defined by $z = k\, xy$. The gaussian and mean

curvatures are hence:

$$G(x,y) = -(k^{-2} + x^2 + y^2)^{-1} \,;\; H(x,y) = -k^3\,xy\,(1 + k^2(x^2 + y^2))^{-3/2} \quad (16)$$

We observe that $H \neq 0$ for non zero x and y: contrary to a common idea, the HP is not a minimal area surface!
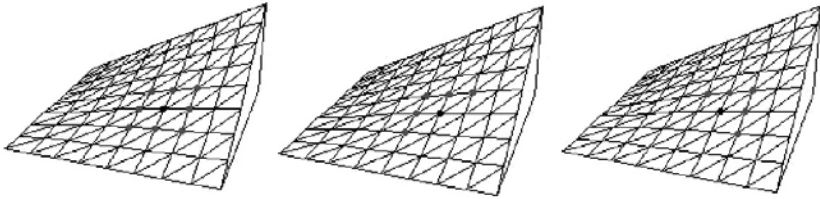

Fig. 16. HP curvatures computation: with R9 (unique possibility) and T6 (several possibilities)

The calculation at one selected point could be envisaged according to different approaches: a quadratic formulation with a R9 rectangle surrounding the point or with a T6 triangle. In that second case, several positioning of the triangle may be used as represented in Fig. 16 (b and c). A cubic interpolation could be as well employed with T10 triangles (not represented).

For R9 element it comes $\xi = \eta = 0$ and $\xi = \eta = 0,5$ for T6. Computations have led to accurate values which are moreover independently on the used element (R9, T6 or T10) and also independently on its positioning in the case of triangles. However, such a result is just a consequence of the HP being a ruled surface. It will not be the same if "non analytic" surfaces (that is to say surfaces which can not be analytically defined) are considered as in the following example.

Membrane example

This application deals with a fabric membrane generated with a shape finding process (force density method, dynamic relaxation...). The aim could be for instance to evaluate some characteristics at one selected point: the maximum curvature radius, the gaussian curvature and the normal vector.

Figure 17 illustrates the several options related to the choice of the element and to its positioning (diverse possibilities excepted for rectangle R9 - a). It is obvious that the associated results will be different and the issue deals with the choice to make.

The problem of positioning may be considered as quite analogous to the stress determination issue at one node after a finite element analysis. Several strategies are indeed achievable: the average value of gauss point values (integration points surrounding the node); the average value of the nodal values obtained on each element comprising the node etc...
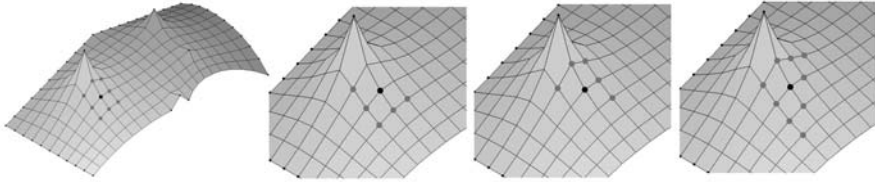
Fig. 17. Different calculation strategies (R9, T6, T6 and T10)

However, we emphasize on the necessity to define approaches based upon the objective of minimal errors. The evaluated geometrical parameter certainly plays a part in the determination of the suitable method.

References

1. Allera R (1992) Mise en forme des structures textiles tendues. Thèse de doctorat, Institut National Polytechnique de Grenoble
2. Barnes MR, Wakefield DS (1988) Form-finding, analysis and patterning of surface-stressed structures. 1st O. Kerensky Memorial Conf., London
3. Bathe KJ (1982) Finite element procedures in engineering analysis. Prentice Hall
4. Dinkler D, Wiedemann B (2001) A finite element concept for wrinkling membranes. Proc. of the IASS symposium, Nagoya,TP04 1–8
5. Ferrari Tissage et Enduction (1989) Rapport documentaire sur les produits
6. Fujiwara J, Ohsaki M, Uetani K (2001) Cutting pattern design of membranes structures considering viscoelasticity of the material. Proc. of the IASS symposium, Nagoya, TP047 1–8
7. Gründig L, Bäuerle J (1990) Automated cutting pattern determination and control for prestressed membranes. Textile Composites in Buil. Cons., part. 2, Ed. Pluralis, 109–120
8. Kim JY, Lee JB (2002) A new technique for optimum cutting pattern generation of membranes structures. Engineering Structures, vol. 24, 745–756
9. Maurin B, Motro R (1999) Cutting pattern with the stress composition method. Int. Journal of Space Structures, vol. 14 N2, 121–129
10. Moncrieff E, Gründig L, Ströbel D (1999) The cutting pattern of the pilgrim's tents for phase 2 of the Mina valley project. Proc. of the IASS 40th anniversary congress, Madrid, C1 129–136
11. Osserman R (1997) Geometry V. Springer Verlag
12. Shimada T, Tada Y (1989) Development of a curved surface using a finite element method. Int. Conf. on Comp. aided optimum Design of Structures, Southampton, 23–30
13. Tsubota H, Yoshida A (1989) Theoretical analysis for determining optimum cutting patterns for membrane structures. IASS Int. Symp. on tensile structures, Madrid, 512–536
14. Xia X, Meek J (2000) Computer cutting pattern generation of membranes structures. Int.Journal of Space Structures, vol 15 N2, 95–110